Hyperthermal neutral beam etching

Konstantinos P. Giapis[a] and Teresa A. Moore
Division of Chemistry and Chemical Engineering, California Institute of Technology, Pasadena, California 91125

Timothy K. Minton[a]
Jet Propulsion Laboratory, California Institute of Technology, Pasadena, California 91109, and Center for Biofilm Engineering and Department of Chemistry and Biochemistry, Montana State University, Bozeman, Montana 59717

(Received 5 October 1994; accepted 6 March 1995)

A pulsed beam of hyperthermal fluorine atoms with an average translational energy of 4.8 eV has been used to demonstrate anisotropic etching of Si. For 1.4 Hz operation, a room-temperature etch rate of 300 Å/min for Si(100) has been measured at a distance of 30 cm from the source. A 14% undercutting for room-temperature etching of Novolac-masked Si features was achieved under single-collision conditions, with no detectable mask erosion. Translational energy and angular distributions of scattered fluorine atoms during steady-state etching of Si by a normal-incidence, collimated beam demonstrate that unreacted F atoms can scatter inelastically, retaining a significant fraction of their initial kinetic energies. The observed undercutting can be explained by secondary impingement of these high-energy F atoms, which are more reactive upon interaction with the sidewalls than would be expected if they desorbed from the surface at thermal energies after full accommodation. Time-of-flight distributions of volatile reaction products were also collected, and they show evidence for a dominant nonthermal reaction mechanism of the incident atoms with the surface in addition to a thermal reaction channel.

I. INTRODUCTION

The ever-decreasing feature dimensions in semiconductor device fabrication have placed unprecedented demands on dry etching technology.[1,2] Most notably, there is an urgent need for a substantial reduction in energetic ion bombardment damage[2] and charge-induced damage,[3,4] occurring during reactive ion etching (RIE). While bombardment damage can in principle be reduced by decoupling the plasma generation means from the processing electrode (typically done with new high-density plasma tools[4]), mitigation of charge-induced damage is inherently more difficult because the very nature of plasmas is based on charged particles. Neutral beams of energetic reactive species have thus been proposed as a way to eliminate both problems simultaneously.[4–10] Collimated beams of hyperthermal neutral atoms or molecules might allow for highly directional etching. Any barrier to etching could be overcome by sufficient translational energy of the etchant species in the beam. If energetic neutral beams are to be useful, it is important first to demonstrate that profile control can be achieved and then to verify damage-free etching of a real device.

Some progress has already been made toward the goal of profile control during etching with neutral beams. Anisotropic etching of semiconductors (Si, GaAs) with a supersonic beam of neutral Cl_2 molecules has been demonstrated.[7–9] In addition, work from the space environmental effects community has shown that a beam of energetic oxygen atoms can etch 0.3-μm-wide features in an organic polymer with insignificant undercutting.[11] An observation common to both types of etching is the existence of a dependence of the etch rate on initial collision energy. Typically, when energy-dependent etching data are fit with an Arrhenius-like expression, activation energies in the range of 0.2–0.4 eV are derived.[8,12,13] In the case of silicon etching with Cl_2, a threshold to etching of 2.0 eV was observed.[9] These findings indicate that practical etching with neutral beams might only be achieved with hyperthermal translational energies; however, in order to avoid bombardment damage, energies should be kept below the threshold for atomic displacement from the crystalline lattice, e.g., 12.9 eV for silicon.[6,14]

The hyperthermal regime of 2–12 eV is not easily accessible. A technique is needed not only to accelerate neutral halogen species to these kinetic energies but also to generate a collimated beam of these species over an area that would permit fabrication of a real chip (>5 cm^2). Conventional supersonic and effusive beam techniques,[7–9] as well as a laser blow-off technique,[15] have been used to study the interaction of neutral species with semiconductor surfaces. Although these experiments reveal much about the interaction mechanisms under the conditions they are studied, the practical range of incident kinetic energies is limited to a few electron volts or less, and the combination of energy and incident flux usually results in too low an etch rate for a study of etch profiles. Furthermore, achievable exposure areas are less than 1 cm^2, making it difficult to fabricate even a prototype device for testing.

We present here a new application of a hyperthermal atomic oxygen source to the production of a halogen-atom beam that can yield practical etch rates over comparatively large areas. Included are operating characteristics of the beam, a demonstration of anisotropic etching, and a preliminary investigation of beam–surface interaction mechanisms. This study reveals etching results within a previously unexplored regime (a directed beam of halogen atoms with hy-

[a]Authors to whom correspondence should be addressed.

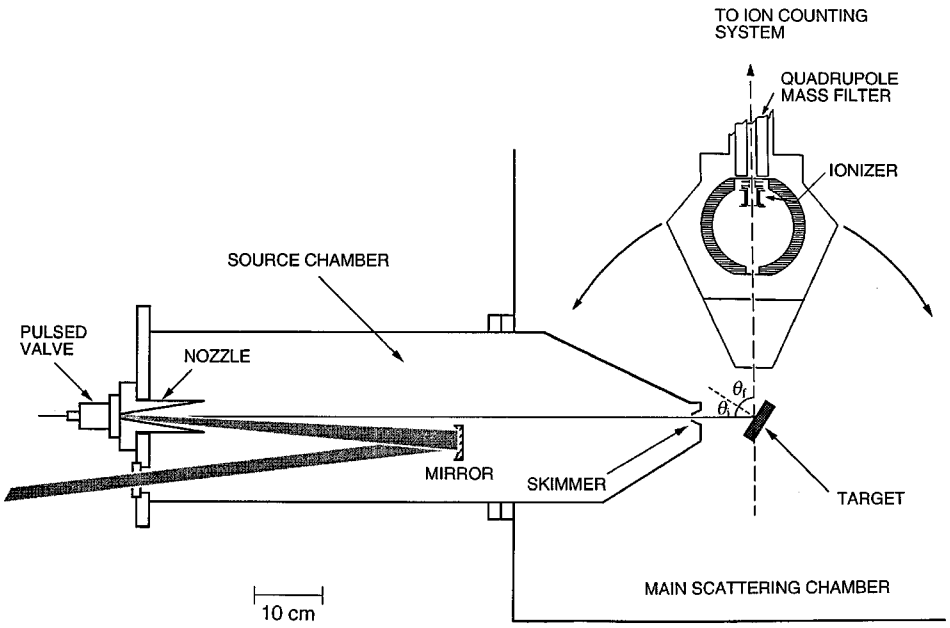

FIG. 1. Schematic depiction of the hyperthermal atom beam source, the differentially pumped scattering region, and the rotatable quadrupole mass spectrometer detector. θ_i and θ_f are the incident and final scattering angles, respectively, defined with respect to the surface normal.

perthermal incident kinetic energies in the range 2–12 eV) and illustrates some important interactions that govern the shape of the etched sidewalls.

II. EXPERIMENTAL DETAILS

Our neutral beam etching studies are based on the coupling of a fast-atom beam source[16] with a crossed molecular beams apparatus.[17] Figure 1 shows a schematic diagram of the essential elements of the apparatus. A pulsed beam of energetic atoms with velocities in the range 4–11 km/s is directed at a target, which can be placed at a variety of distances from the source. At one of the target positions, 92 cm from the apex of the conical nozzle source, the target and a mass spectrometer detector can be rotated about the same axis; therefore, inelastic and reactive species emerging from the target surface during etching can be detected, and the velocities and intensities of these volatile species can be measured as a function of incident and final scattering angles θ_i and θ_f. The detector can also be positioned such that the detection axis coincides with the beam axis in order to determine the species in the beam and their velocities.

The beam source is based on the laser detonation source described in Ref. 16. We focus the light pulse from an Alltec model 851 CO_2 TEA laser into a 10-cm-long, water-cooled copper nozzle by means of a gold mirror placed 50 cm from the apex of the cone. A home-built piezoelectric pulsed molecular beam valve[18] is used to inject pure SF_6 gas, at a stagnation pressure of 125 psig, into the nozzle cone through a 1-mm-diam orifice at the apex. The SF_6 gas is atomized in the laser-induced plasma, and, following electron-ion recombination in the expanding, high-density plasma, a nominally neutral beam of high-velocity atomic fluorine and sulfur emerges. The beam has a nominal direction, determined by the 20° full included angle of the conical nozzle; however, the angular divergence of the beam can be significantly reduced with the use of an aperture. We estimate the F-atom beam flux on axis 30 cm from the nozzle apex to be approximately 2×10^{15} atoms/cm^2/pulse.[19] Previous results with an atomic oxygen beam have shown that the average beam flux on axis, as determined from the erosion yield of a polymer, is proportional to the inverse square of the distance from the source;[13] thus, the estimated average atomic fluorine flux at the position of the detector rotation axis is 2×10^{14} atoms/cm^2/s.

Characterization of the hyperthermal beam was performed by aligning the detector and beam axes and collecting signal at various mass-to-charge ratios (m/e) as a function of time following the laser detonation pulse. These beam time-of-flight (TOF) distributions $N(t)$ were used to derive translational energy distributions $P(E)$ for the various species in the beam pulse that traveled 126.5 cm from the nozzle apex to the detector ionizer.[20,21] A beam TOF distribution $N(t)$, collected at $m/e=19$ with the mass spectrometer directly viewing the beam, is shown in Fig. 2(A); Fig. 2(B) shows the corresponding translational energy distribution $P(E)$. The average translational energy of the F atoms in the beam was 4.8 eV, and the energy spread [full width at half-maximum (FWHM)] was ~3.0 eV. The respective quantities for the sulfur component of the beam were 8.2 and 5.5 eV. While these beam characteristics apply to the experiments described here, the average F-atom kinetic energy can be varied easily over the range 3–7 eV by adjusting the valve-laser timing and the stagnation pressure of the gas behind the nozzle.

The beam composition was investigated by collecting TOF distributions at all masses that showed beam-modulated signal. The mass spectrum, shown in Fig. 3, demonstrates that the beam consisted almost entirely of atomic fluorine and sulfur.[22] The relative ion content of the beam was determined to be negligible by comparing the signals at various

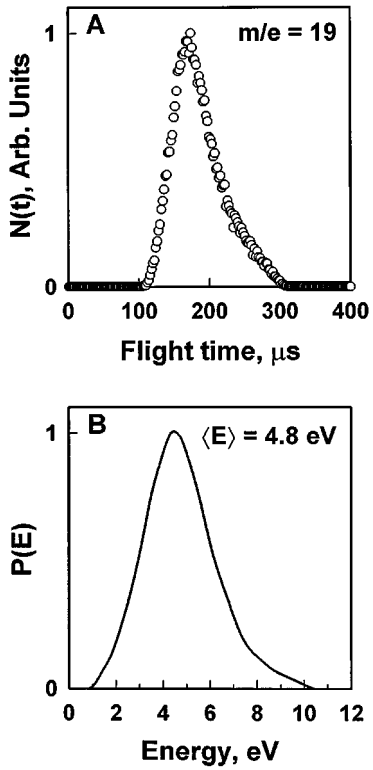

FIG. 2. (A) Beam time-of-flight distribution collected at $m/e=19$ (F^+). Time zero corresponds to the firing of the laser pulse. (B) Translational energy distribution of F atoms in beam, derived from the TOF distribution in (A).

masses with the ionizer turned on to those with the ionizer turned off. At $m/e=19$, the integrated signal with the ionizer off dropped to less than one percent of the value measured with the ionizer on. We thus concluded that the ion fraction in the beam must have been $\ll 1\%$ because neutrals are ionized with an efficiency of $\sim 10^{-4}$ in our modified Brink-type ionizer.[17(a)] We cannot rule out the possibility that metastable atoms are present in the beam. Metastable fluorine atoms have been detected at times as long as 35 μs following electron impact excitation of SF_6,[23] and some metastables could have lifetimes greater than 100 μs.[24] Even though metastable atoms are probably formed in our source, the local pressure during the laser-sustained discharge may lead to efficient electronic quenching[25] before the atoms exit the source region.

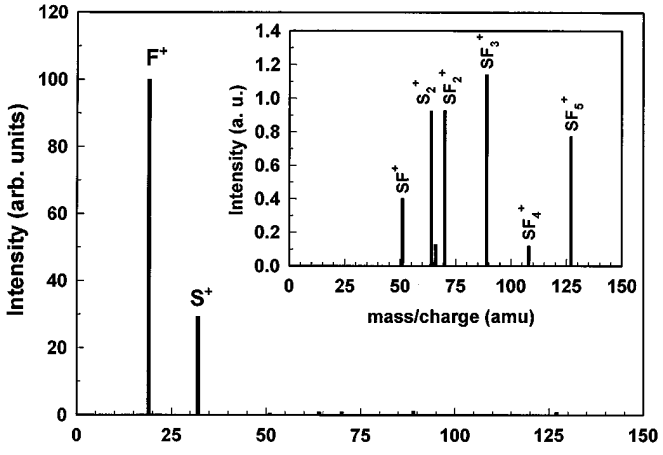

FIG. 3. Mass spectrum of hyperthermal beam, obtained from integrated beam time-of-flight distributions.

Two types of experiments were performed with the hyperthermal beam described above operating at 1.4 Hz: (1) Masked, semi-insulating silicon wafers, kept at room temperature, were etched in the beam path at distances of 30 cm (in the source chamber) and 92 cm (in the scattering chamber) from the nozzle apex, and (2) TOF distributions of products scattered inelastically and reactively from an n-type, epitaxial Si(100) surface[26] (held at 345 K and situated 92 cm from the source) were monitored with the rotatable mass spectrometer detector. All etching experiments consisted of exposure of the masked wafers to the atomic beam at normal incidence ($\theta_i=0°$). Scattering data were collected at a variety of incident and final angles (see Fig. 1), after reaching steady-state etching conditions, as determined from the reproducibility in the shape of the TOF distributions. At the 92 cm nozzle–surface distance, the beam diameter was reduced as a result of its passage through a 25-mm-diam orifice (etching experiment) or a 3-mm-diam skimmer (scattering experiment) both of which were placed 85 cm from the nozzle apex. The aperture was the dividing line between two differentially pumped regions of the apparatus. The source chamber, pumped by a 10 in. diffusion pump with an ethanol-cooled baffle kept at -27 °C, had an ultimate pressure of 2×10^{-6} Torr and went up to approximately 1 mTorr during the beam pulse. The main scattering chamber was pumped by two 10 in. cryopumps and a liquid-nitrogen cryopanel and had an ultimate pressure of 1×10^{-7} Torr. The pressure in this chamber rose to 2×10^{-6} Torr during the beam pulse with the larger aperture and 2×10^{-7} Torr with the smaller aperture. 81 000 pulses were used to etch the wafer at the 92 cm position, and a variety of exposure durations, all $<80\,000$ pulses, were used to etch wafers at the 30 cm position. Typical counting times for the TOF distributions of scattered species were 200–1000 pulses. The time resolution of the TOF distributions was determined by the width of the incident beam pulse. The TOF distributions presented in this article have been corrected for the ion flight time in the detector, 2.3 $(m/e)^{1/2}$ μs.

III. ETCHING RESULTS

The scanning electron micrograph (SEM) in Fig. 4 shows a cross-sectional view of trenches that were etched into a masked Si wafer[27] placed 92 cm from the nozzle. The shape of the mask was a result of incomplete clearing in an oxygen plasma; no observable alteration (erosion, sputtering) of the mask occurred even after etching to a depth of 5 μm. The room-temperature etch rate observed at the 92 cm position was 10 Å/min. The profiles were undercut by 14%, which is comparable to what is expected and seen in RIE of Si at room temperature with fluorine-based chemistry and no simultaneous deposition on the sidewalls.[28] We also observed features typically seen in RIE profiles, such as microtrenching and dovetailing;[2] however, in contrast with typical RIE profiles, the features in Fig. 4 also exhibit ''inverse microloading,'' or a higher etch rate between two closely spaced

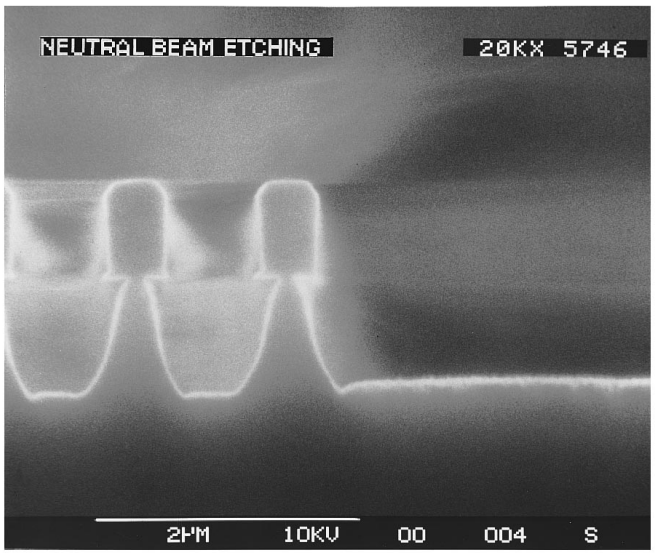

FIG. 4. SEM cross-sectional view of trenches in Si etched by the hyperthermal neutral F atom beam to a depth of approximately 0.9 μm. Reentrant mask shape is due to mask definition in an oxygen plasma; no mask erosion occurred during the hyperthermal beam processing.

features than in an open area away from masked features. The surface appearance after etching was rough (grainy) with an average grain size of approximately 50 nm for an etch depth of 1 μm. We have also etched the same structures in the source chamber at a distance of 30 cm from the nozzle apex, where the profiles (not shown here) were undercut by 50% and the etch rate was 300 Å/min, a much higher etch rate than would have been expected by the inverse square dependence on the beam flux.

This unexpectedly high etch rate might arise from a nonlinear flux dependence and/or a high ambient F-atom pressure in the source chamber during the pulse. The ambient pressure in the source chamber increases significantly during the beam pulse, so a wafer placed in this region is subject to continued spontaneous etching from thermal F atoms after the initial hyperthermal pulse has dissipated but before the chamber is thoroughly evacuated. Any contribution from such spontaneous etching would enhance undercutting and material removal rate.

A high local pressure at the surface during the beam pulse could also contribute to undercutting. The relatively high beam flux at the 30 cm position can result in a pressure buildup at the surface, especially in confined regions between features. Gas-phase scattering of the slower portion of the beam pulse could then lead to more isotropic etching.

The origin of the undercutting is important because of its implications for anisotropic etching by directed fast neutral beams[6,8] and also because of its relevance to RIE.[28,29] In our experiment, the undercutting at the 92 cm position is particularly relevant to the ultimate potential of neutral beam etching because the beam of neutral F atoms interacted with the Si surface under conditions where gas-phase scattering was negligible and background pressure was low. Therefore, the undercutting must be the result of one or more surface mediated processes. In RIE profiles, undercutting has been commonly attributed to thermal desorption[6,8,29] and surface diffusion[30] of unreacted fluorine atoms from the bottom of the trenches. Singh *et al.*[29] explored these processes in a model of the profile evolution during RIE in an SF_6 plasma. Their simulation was based on a fit of one experimental profile which determined the value of the sticking probability as well as the neutral-to-ion flux ratio on the etched surface. They discounted surface diffusion because they found that it would require an unreasonably long time scale in order to be an important mechanism in profile evolution. Nevertheless, they were able to predict etch profiles by considering contributions from thermal desorption alone. However, their fitting procedure resulted in a very low sticking probability of 0.01 and led to the conclusion that, in order to predict the substantial undercutting, a very large number of unreacted fluorine atoms must leave the surface at thermal energies. While a sticking probability of 0.01 is expected when spontaneous etching takes place, ion bombardment during RIE facilitates a reduction in surface coverage which in turn leads to an increased sticking probability.[31] An alternative explanation suggests that this unrealistic modeling result for the highly reactive F+Si system may be unnecessary. The undercutting may occur even when the sticking probability is much higher than 0.01 if the unreacted fluorine atoms have *higher* translational energies than expected from a Maxwell–Boltzmann distribution and are, therefore, more reactive upon impact with the sidewalls. Higher translational energies could result from nonthermal (direct) inelastic scattering,[32–35] where an incoming atom retains memory of the incidence conditions. The contribution of direct inelastic scattering to undercutting has received little attention in relation to etching.

IV. SCATTERING DYNAMICS

Figure 5 shows a representative set of TOF distributions taken at $\theta_i=0°$ and $\theta_f=47°$ for five masses corresponding to reactive products and one mass ($m/e=19$) corresponding to inelastically scattered F atoms, which emerge from the surface without reaction.[36] The scattered fluorine atoms have an average translational energy substantially higher than that expected from a Maxwell–Boltzmann distribution, indicating that thermal desorption accounts only for a minor fraction of unreacted F atoms. Indeed, the $m/e=19$ TOF distribution of Fig. 5 implies a peak translational energy of 0.32 eV for the scattered F atoms exiting at $\theta_f=47°$. This value increases to 0.38 eV for F atoms scattered at $\theta_f=62°$, the largest exit angle monitored. The surface temperature would have to be in the range 2500–3000 K in order to impart desorbing atoms with kinetic energies in this range. The surface was, in fact, kept at 345 K during the interaction. Furthermore, the shape of all $m/e=19$ TOF distributions indicates that the velocity distribution of F atoms emerging from the surface is not Maxwell–Boltzmann. Finally, the angular distribution of scattered F atoms is not cosine, as would be expected for thermally desorbed F atoms. Therefore, most unreacted fluorine atoms must scatter from the surface via a nonthermal process and thus retain a significant fraction of their incident energies. This fraction increases at larger scattering angles. For example, at the largest scattering angles

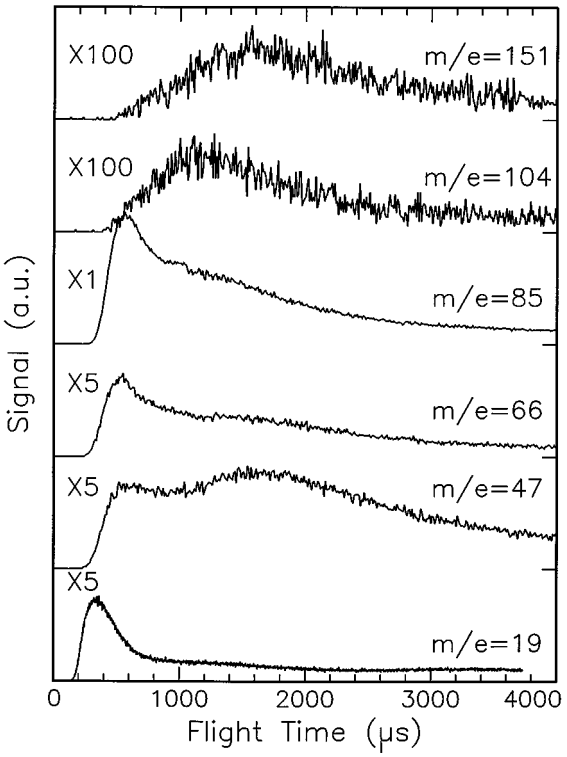

FIG. 5. Time-of-flight distributions of inelastically scattered fluorine ($m/e=19$) and reactive products detected at the various m/e ratios indicated, taken for $\theta_i=0°$ and $\theta_f=47°$ with a surface temperature of 345 K. Time zero corresponds to the firing of the laser pulse.

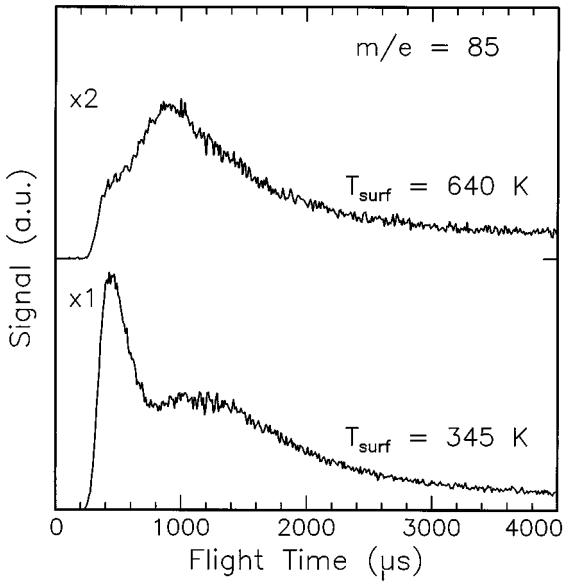

FIG. 6. Time-of-flight distributions collected at $m/e=85$ for the two temperatures indicated. The incident and final angles were $\theta_i=60°$ and $\theta_f=62°$. Time zero corresponds to the firing of the laser pulse.

monitored ($\theta_i=60°$ and $\theta_f=62°$), the peak in the TOF distribution corresponds to F atoms with 2.9 eV of translational energy, which is 60% of the incident energy.

Although the initial interaction results in three-dimensional scattering, the TOF distributions of Fig. 5 give an idea of the relative magnitude of the F-atom signal in the scattering plane. When converted to a flux distribution from a number density distribution[20] and corrected for relative ionization cross sections and number of fluorine atoms in each detected product species, the TOF distributions reveal that the flux of inelastically scattered F atoms is roughly 65% of the flux of F atoms contained in reactive products exiting the surface at $\theta_f=47°$. Other combinations of incident and final angles also show substantial scattered flux of unreacted F atoms in the scattering plane. Our scattering data therefore support the conclusion that undercutting comes from secondary impingement of energetic fluorine atoms which scatter inelastically upon initial impact with the fluorinated Si surface. If the impinging F atoms encountered a virgin Si surface or one with reduced surface coverage, they would be more likely to react,[31] and undercutting resulting from inelastic scattering should be diminished.

The TOF distributions of the reactive products detected at $m/e=85$, 66, 47 are bimodal, suggesting that at least two interaction mechanisms with the surface lead to ejection of volatile reaction products. The slower component (longer arrival times) at each mass can largely be explained by ionizer fragmentation of heavier products which are traveling at velocities corresponding to the surface temperature. For example, the slower component of the $m/e=85$ (SiF_3^+) TOF distribution has approximately the same arrival time and shape as the $m/e=104$ (SiF_4^+) TOF distribution. This observation and the relatively high SiF_3^+ signal are consistent with the conclusions of earlier experiments[10,37] that SiF_4 products exit the surface at thermal energies and fragment in the ionizer to give a dominant mass peak at $m/e=85$. The faster, or hyperthermal, component (short arrival times) at $m/e=85$ has no corresponding peak at $m/e=104$ or 151 (heavier products were not detected). Unless a product heavier than 85 amu happens to exit the surface at hyperthermal velocities and fragment much more in the ionizer than the same product exiting at thermal velocities, then the hyperthermal component at $m/e=85$ must originate from an SiF_3 reaction product. The hyperthermal signal seen at lower masses may come from a combination of ionizer fragmentation of SiF_3 and direct ejection of SiF_2 and SiF products. While the detailed reaction mechanisms giving rise to the two components observed in the TOF distributions are unclear, it is clear that (a) thermal and nonthermal interactions are taking place at the surface and (b) the dominant reactive signals are the result of one or more nonthermal processes.

The dependencies of the nonthermal signal on scattering angle and surface temperature provide clues to its origin. Figure 6 shows $m/e=85$ TOF distributions collected at $\theta_i=60°$ and $\theta_f=62°$ for two surface temperatures, 345 and 640 K. The fast peak in the TOF distribution of products emerging from the lower-temperature sample corresponds to an SiF_3 translational energy of ~0.60 eV. In contrast, the peak translational energy derived from the $m/e=85$ TOF distribution in Fig. 5 (where $\theta_i=0°$ and $\theta_f=47°$) is ~0.31 eV. In general, we have observed angular dependencies on translational energy for the hyperthermal reactive and nonreactive products that mirror the scattering of energetic rare gas atoms from liquid surfaces:[35] the translational energy of the

scattered species increases with increasing total included scattering angle $(\theta_i+\theta_f)$. For a reactive process, this behavior could be indicative of either a direct (Eley–Rideal) reaction[38] or collision induced desorption.[39,40] The large decrease in the nonthermal reactive signal when the surface temperature is increased (see Fig. 6) could result from either mechanism if a temperature increase makes thermal desorption of the appropriate collision partner more competitive with the reactive processes taking place on the surface during interaction with the beam pulse. More work must be done in order to distinguish between the possible mechanisms and to determine what role, if any, metastable atoms play in the beam–surface interaction. It should be noted that the existence of a nonthermal, collision-cascade mechanism in connection with ion-assisted etching has been reported and debated in the literature.[41,42] Also, Szabó *et al.* have recently proven that collision-induced desorption plays a role in the reaction of chlorine with silicon.[43] Although not typically observed, nonthermal processes, such as direct reaction and collision-induced desorption, could be important in the regime of high incident energy and instantaneous flux, where we are studying neutral beam etching.

During the scattering experiments, no SiS_x products were detected in the mass spectrometer. Furthermore, after the experiment, the exposed surface was examined by x-ray photoelectron spectroscopy (after air transfer), and no sulfur was detected. Therefore, we concluded that sulfur atoms did not react with the surface. Their role in etching due to energy transfer during bombardment of the surface might, however, be important.

V. SUMMARY AND CONCLUSIONS

A neutral beam of hyperthermal fluorine atoms, produced by laser detonation of SF_6 and possessing an average translational energy of 4.8 eV, has been used to etch submicron features in silicon. We observed 14% undercutting for etching at room temperature and concluded from scattering experiments that the undercutting resulted largely from fluorine atoms scattering inelastically at hyperthermal velocities from the fluorinated silicon surface. Angle- and velocity-resolved measurements demonstrated that fluorine atoms can retain a fraction of their incident energy even after head-on collisions with the etched surface and suggest that secondary impingement of energetic etchant species should be included in modeling studies of profile evolution. A significant flux of energetic reaction products (e.g., SiF_3) might also need to be considered as a source of undercutting if they themselves are reactive. Finally, some TOF distributions of reactive products are bimodal, suggesting the existence of at least two reactive processes at the surface, one thermal and the other nonthermal.

These experiments imply that improved anisotropy will be achieved by reducing the reactivity and flux of scattered reactive species. Approaches that can be considered include (a) increasing the mass of the etchant species to enhance energy transfer during the initial interaction so that inelastically scattered species carry less energy to the sidewalls; (b) increasing the reactivity during the first encounter of the etchant species with the surface so that the flux of the scattered reactive species is reduced; (c) reducing the surface temperature and thus reactivity so that the energy of the scattered species is not enough to facilitate reaction at the sidewalls; (d) reducing the translational energy of the incident beam in order to lower the energy of the scattered reactive species; and (e) choosing an etchant species that requires more translational energy to react.

ACKNOWLEDGMENTS

This work was carried out at the Jet Propulsion Laboratory (JPL), California Institute of Technology, under contract with the National Aeronautics and Space Administration (NASA). This research was supported by the Ballistic Missile Defense Organization/Innovative Science and Technology Office and by NASA through a grant from the JPL Director's Discretionary Fund. The authors are grateful to Dr. Charles W. Jurgensen at AT&T Bell Laboratories for supplying masked silicon wafers for this experiment. One of the authors (K.P.G.) thanks the Camille and Henry Dreyfus Foundation for a New Faculty award.

[1] J. M. Cook and K. G. Donohoe, Solid State Technol. 119, April 1991.
[2] R. A. Gottscho, C. W. Jurgensen, and D. J. Vitkavage, J. Vac. Sci. Technol. B **10**, 2133 (1992).
[3] C. T. Gabriel and J. P. McVittie, Solid State Technol. 81, June 1992.
[4] T. Mizutani and T. Yunogami, Jpn. J. Appl. Phys. **29**, 2220 (1990).
[5] M. W. Geis, N. N. Efremow, S. W. Pang, and A. C. Anderson, J. Vac. Sci. Technol. B **5**, 363 (1986).
[6] K. Suzuki, S. Hiraoka, and S. Nishimatsu, J. Appl. Phys. **64**, 3697 (1988).
[7] F. Shimokawa, H. Tanaka, Y. Uenishi, and R. Sawada, J. Appl. Phys. **66**, 2613 (1989).
[8] T. Ono, H. Kashima, S. Hiraoka, and K. Suzuki, J. Vac. Sci. Technol. B **9**, 2798 (1991).
[9] Y. Teraoka and I. Nishiyama, Appl. Phys. Lett. **63**, 3355 (1993).
[10] H. F. Winters and J. W. Coburn, Surf. Sci. Rep. **14**, 161 (1992).
[11] S. Koontz and J. Cross, NASA Tech Briefs MSC-21631, 86, February 1993.
[12] J. B. Cross, S. L. Koontz, and E. H. Lan, in Proceedings of the 5th International Symposium on Materials in the Space Environment, Cannes, France, September 1991 (unpublished).
[13] R. H. Krech, NASA Final Report, Prepared under Contract No. NAS3-25968 by Physical Sciences, Inc., Andover, MA, March 1993.
[14] G. Carter and J. S. Coligon, *Ion Bombardment of Solids* (Heineman, London, 1968), p. 214.
[15] F. X. Campos, G. C. Weaver, C. J. Waltman, and S. R. Leone, J. Vac. Sci. Technol. B **10**, 2217 (1992).
[16] G. E. Caledonia, R. H. Krech, and D. B. Green, AIAA J. **25**, 59 (1987); U.S. Patent No. 4 894 511 (16 January 1990).
[17] (a) Y. T. Lee, J. D. McDonald, P. R. LeBreton, and D. R. Herschbach, Rev. Sci. Instrum. **40**, 1402 (1969); (b) M. J. O'Laughlin, B. P. Reid, and R. K. Sparks, J. Chem. Phys. **83**, 5647 (1985).
[18] D. Proch and T. Trickl, Rev. Sci. Instrum. **60**, 713 (1989).
[19] This estimate is based on a comparison of F-atom signal intensity registered at $m/e=19$ with the O-atom intensity ($m/e=16$) from a beam of hyperthermal atomic oxygen whose flux was calibrated from an erosion measurement of Kapton polyimide polymer, which has a known reactivity of 3×10^{-24} cm^3/atom.
[20] The mass spectrometer is a number density detector. Therefore, the derivation of the flux through the detector as a function of time $I(t)$ must take into account the residence time in the ionizer. In particular, an inverse time correction must be applied to the measured TOF distributions [i.e., $I(t)\propto N(t)/t$]. The probability of a species possessing a given translational energy is proportional to the flux [$P(E)dE\propto I(t)dt$], which leads to the relationship $P(E)\propto t^2N(t)$ between the translational energy and TOF distributions.
[21] The contribution of the high velocities of the neutral species to the resulting ion energies in the detector could manifest itself as a dependence of

the detector efficiency on the flight time. However, we found the detection efficiency to be virtually independent of ion energy in the 10 eV range above the nominal ion energy employed (58 eV), so the observed TOF distributions were assumed to be accurate reflections of the respective translational energy distributions for the detected species.

[22]Not only did the SF_n fragments give weak signals in the detector, but they traveled at relatively slow velocities and thus produced signal at much longer flight times (with maxima near 280 μs) than the fluorine-atom signal detected at $m/e=19$ [cf Fig. 2(A)]. Hence, any contribution of the SF_n fragments to the signal at $m/e=19$ through ionizer fragmentation must be inconsequential. This same conclusion applies to the sulfur-atom signal detected at $m/e=32$.

[23]J. J. Corr, M. A. Khakoo, and J. W. McConkey, J. Phys. B **20**, 2597 (1987).

[24]V. Vujnovic and M. L. Burshtein, Astron. Astrophys. **151**, 442 (1985).

[25]S. G. Hansen, G. Luckman, G. C. Nieman, and S. D. Colson, Appl. Phys. Lett. **56**, 719 (1990).

[26]The sample cleaning procedure involved degreasing for 10 min in boiling trichloroethylene followed by 10 min in boiling ethanol (200 proof USP), a dip in nanopure H_2O, followed by etching for 15 s in conc HF (49%), a rinse in nanopure H_2O, and finally a dip in boiling ethanol. The sample was transferred in air to the scattering chamber.

[27]The masked Si wafer was produced by trilayer photolithography. The remaining mask on the wafer consisted of Novolac photoresist and was defined by etching in an oxygen plasma. The trenches did not clear thoroughly, and a sharp edge of resist could be seen in SEM pictures of the wafer.

[28]D. L. Flamm, in *Plasma Etching*, edited by D. M. Manos and D. L. Flamm (Academic, Boston, 1989), Chap. 2.

[29]V. K. Singh, E. S. G. Shaqfeh, and J. P. McVittie, J. Vac. Sci. Technol. B **10**, 1091 (1992).

[30]M. Sato, S. Kato, and Y. Arita, Proceedings of the 12th Symposium on Dry Processes, Tokyo, Japan, 1990 (unpublished), p. 123.

[31]Y. Y. Tu, T. J. Chang, and H. F. Winters, Phys. Rev. B **23**, 823 (1981).

[32]J. Harris, in *Dynamics of Gas-Surface Interactions*, edited by C. T. Rettner and M. N. R. Ashfold (The Royal Society of Chemistry, Cambridge, England, 1991), Chap. 1.

[33]C. T. Rettner, J. A. Barker, and D. S. Bethune, Phys. Rev. Lett. **67**, 2183 (1991).

[34]M. E. Saecker, S. T. Govoni, D. V. Kowalski, M. E. King, and G. M. Nathanson, Science **252**, 1421 (1991).

[35]M. E. King, G. M. Nathanson, M. A. Hanning-Lee, and T. K. Minton, Phys. Rev. Lett. **70**, 1026 (1993).

[36]The signal collected at $m/e=19$ may contain contributions from ionizer fragmentation of Si_xF_y reactive products. However, the majority of the $m/e=19$ signal most likely comes from unreacted fluorine atoms, because much of this signal arrives at shorter flight times than signal from the heavier masses and also because the probability for Si_xF_y products to lead to F^+ in the ionizer is expected to be low.

[37]H. F. Winters and I. C. Plumb, J. Vac. Sci. Technol. B **9**, 197 (1991).

[38]E. W. Kuipers, A. Vardi, A. Danon, and A. Amirav, Phys. Rev. Lett. **66**, 116 (1991); Surf. Sci. **26**, 299 (1992); W. H. Weinberg, in Ref. 32, Chap. 5; C. T. Rettner and D. J. Auerbach, Science **263**, 365 (1994).

[39]Y. Zeiri, J. J. Low, and W. A. Goddard III, J. Chem. Phys. **84**, 2408 (1986).

[40]J. D. Beckerle, A. D. Johnson, and S. T. Ceyer, J. Chem. Phys. **93**, 4047 (1990); S. T. Ceyer, Science **249**, 133 (1990).

[41]R. A. Haring, A. Haring, F. W. Saris, and A. E. de Vries, Appl. Phys. Lett. **41**, 174 (1982).

[42]F. A. Houle, Appl. Phys. Lett. **50**, 1838 (1987).

[43]A. Szabó, P. D. Farrall, and T. Engel, J. Appl. Phys. **75**, 3623 (1994).